Supplementary material

Revisiting the three largest surface ozone episodes in Europe during 2003–2022 using circulation analogues

Tahimy Fuentes-Alvarez[a,*], Carlos Ordóñez[a], Ricardo García-Herrera[a,b], David Barriopedro[b], Jose M. Garrido-Perez[a]

[a] Departamento de Física de la Tierra y Astrofísica, Facultad de Ciencias Físicas, Universidad Complutense de Madrid, Madrid, Spain

[b] Instituto de Geociencias (IGEO), Consejo Superior de Investigaciones Científicas-Universidad Complutense de Madrid (CSIC-UCM), Madrid, Spain

* Corresponding author. E-mail address: tahifuen@ucm.es

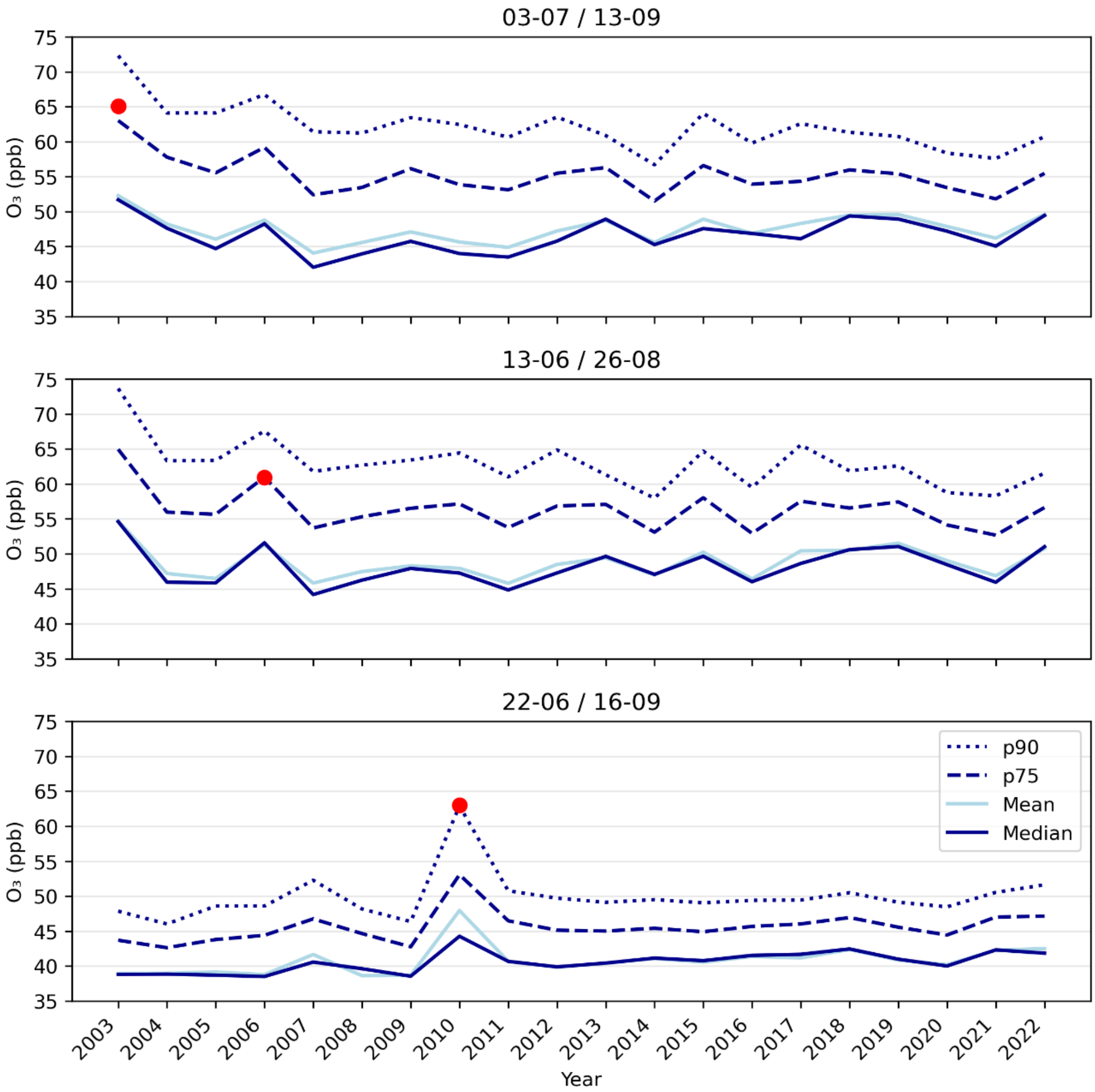

Figure S1. Evolution of key statistics of the daily maximum ozone mixing ratios over the target regions (black boxes of Figure 1 in the main text) during the 3 July – 13 September (top), 13 June – 26 August (middle) and 22 June – 16 September (bottom) periods of 2003–2022. These time spans have been used to include periods that cover from 30 days before the beginning to 30 days after the end of each ozone episode (August 2003 and July 2006 in western Europe, and July – August 2010 in western Russia, respectively). The dark blue and light blue solid lines represent the median and mean values, respectively, while the dashed and dotted lines denote the 75th and 90th percentiles. Red dots indicate the regional average of the daily maximum ozone mixing ratios calculated over the same boxes considering only the days of each episode (2–14 August 2003, 13–27 July 2006 and 22 July–17 August).

.

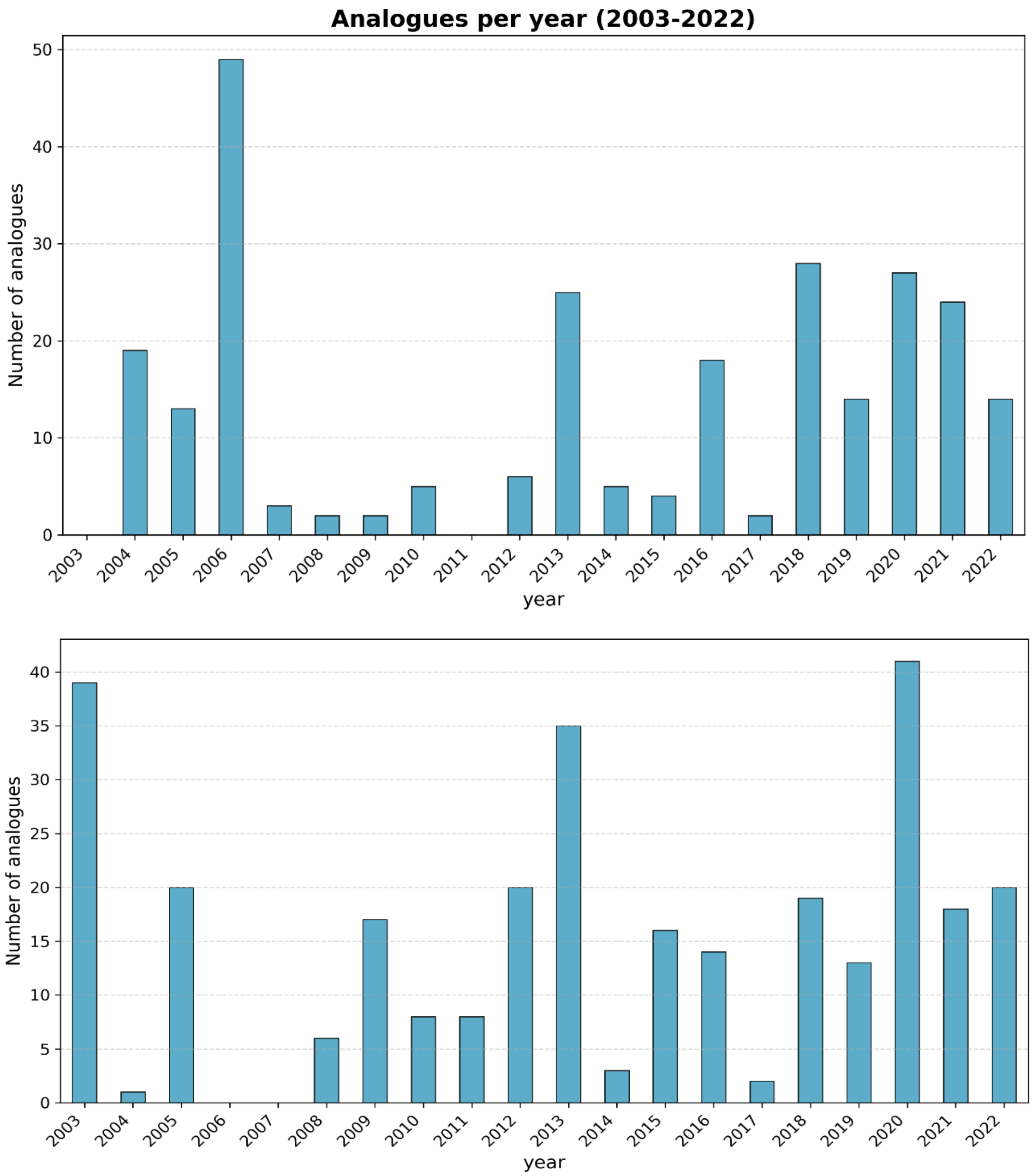

Figure S2. Number of flow analogues per year obtained for the days of the (top) 2–14 August 2003 and (bottom) 13–27 July 2006 ozone episodes that affected western Europe.

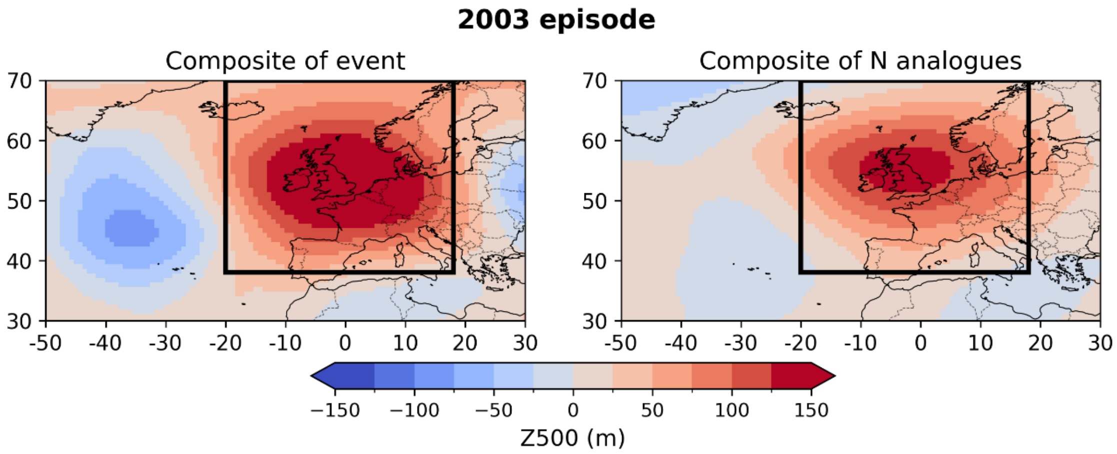

Figure S3. Composite of daily detrended Z500 anomalies during the August 2003 episode (left) and the corresponding circulation analogue days (right).

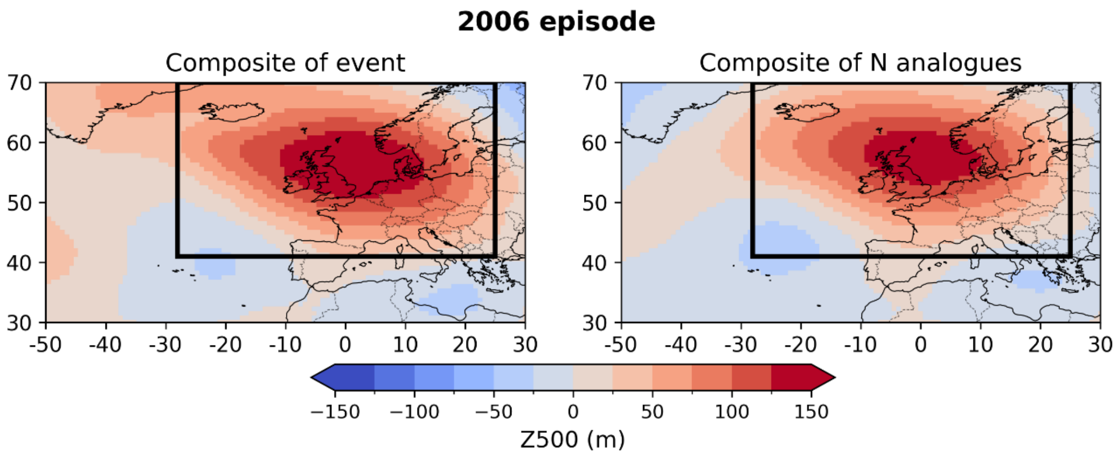

Figure S4. As Figure S3, but during the July 2006 episode (left) and the corresponding circulation analogue days (right).

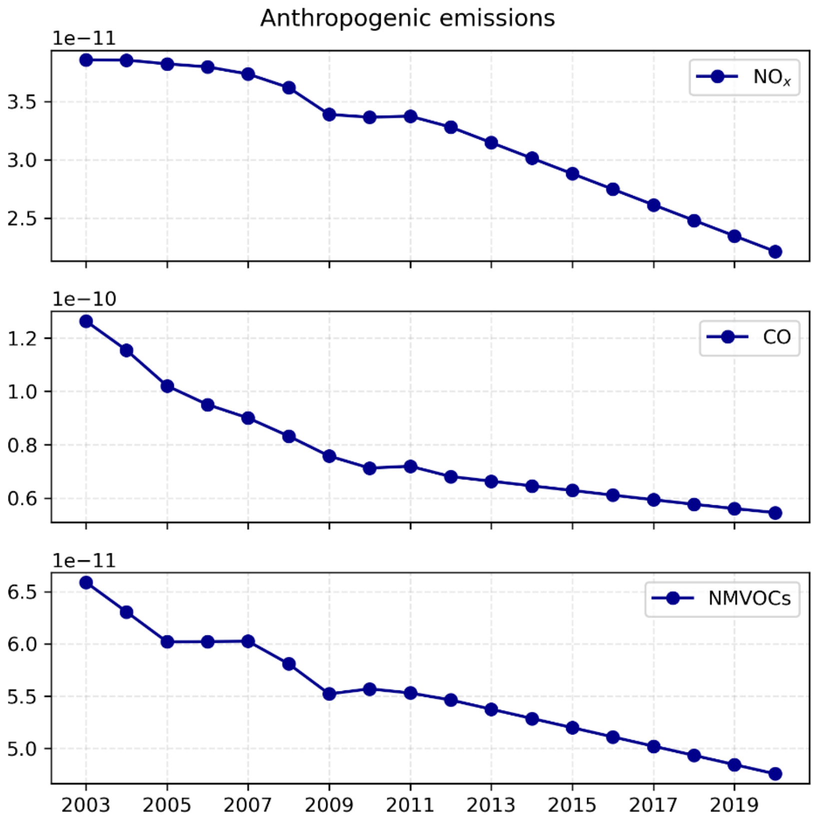

Figure S5. Time series of July–August anthropogenic emissions of ozone precursors (kg m^{-2} s^{-1}), averaged over all grid cells within the dashed blue boxes over western Europe [35°–55° N, 7° W–19° E] in Fig. 1 (left and middle panels) of the main text: (top) NO_x, (middle) CO and (bottom) NMVOCs.

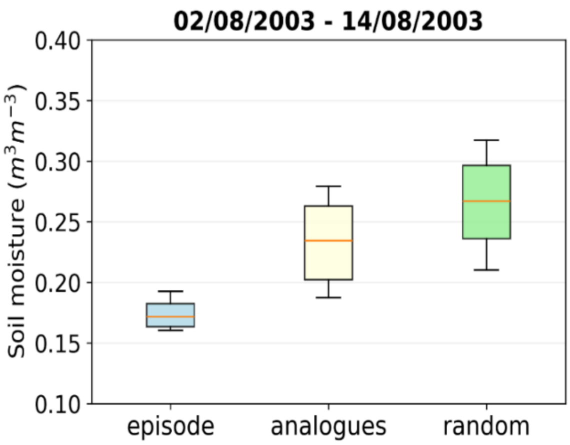

Figure S6. Distributions of regional average volumetric moisture content in the upper soil layer (0–7 cm) over the target region during (blue) the days of the August 2003 episode, as well as (yellow) analogue days and (green) random days for the same episode.

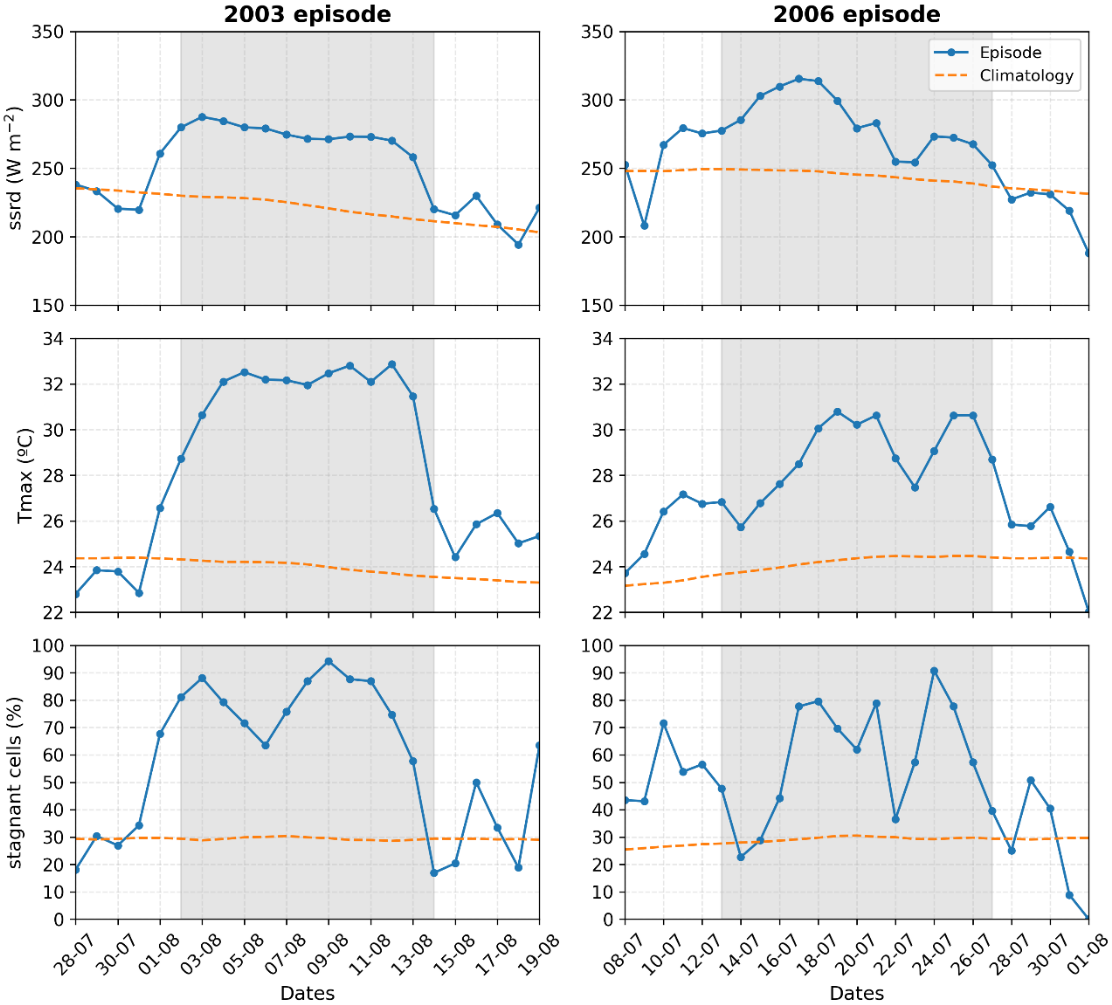

Figure S7. Evolution of daily mean values averaged over the target regions from 5 days before to 5 days after the 2-14 August 2003 (left column) and 13-27 July 2006 (right column) episodes for surface net solar radiation (ssrd, top), daily maximum temperature (Tmax, middle) and the percentage of stagnant grid cells (bottom). Grey shading delineates the duration of the Aug 2003 and Jul 2006 episodes.

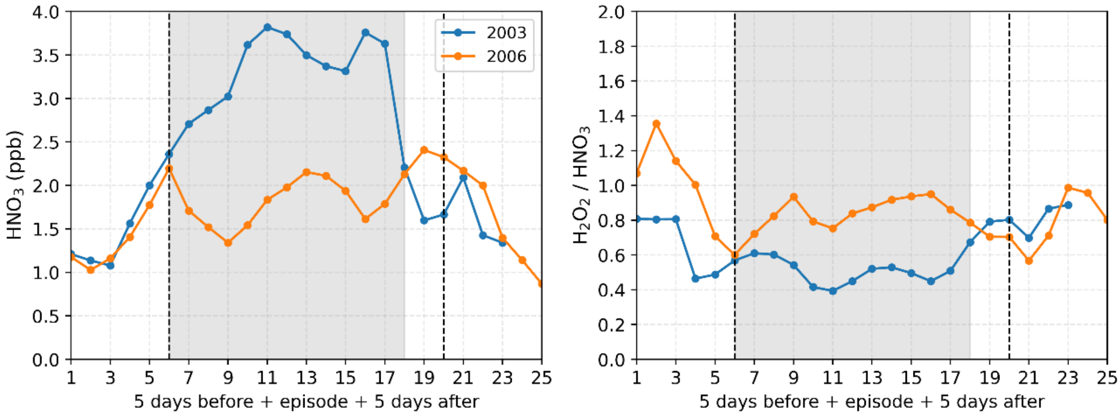

Figure S8. Evolution of HNO_3 mixing ratios (left) and the H_2O_2/HNO_3 concentration ratio (right), averaged over the target regions from 5 days before to 5 days after the 2-14 August 2003 (blue) and 13-27 July 2006 (orange) episodes. Values are calculated as averages of daytime data (12 and 15 UTC) for each day. Grey shading and vertical dashed lines delineate the duration of the Aug 2003 and Jul 2006 episodes, respectively.

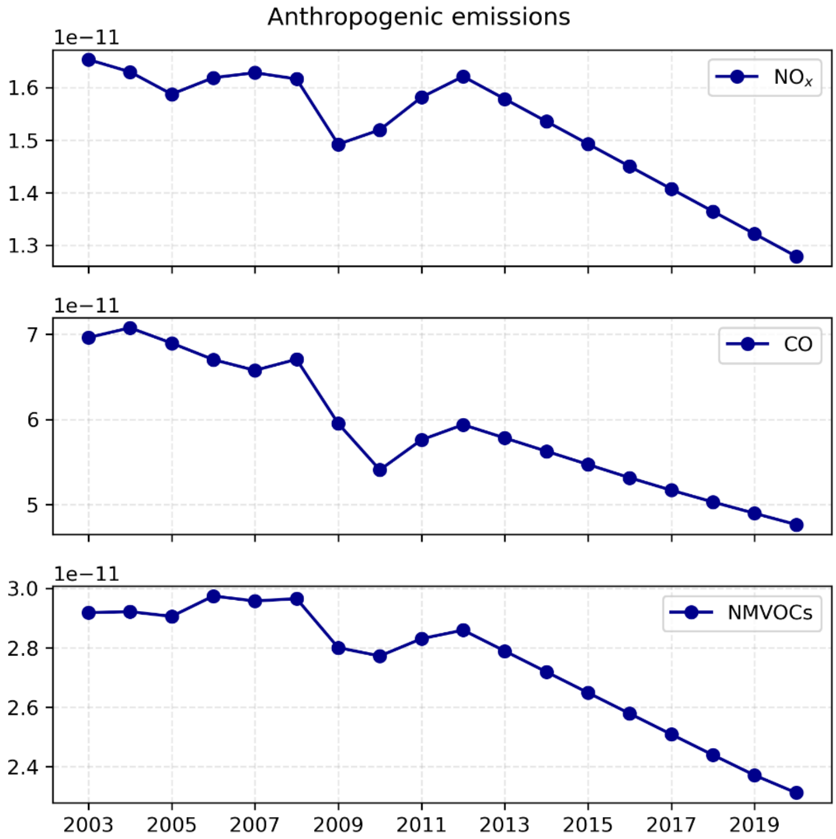

Figure S9. As Figure S5 but averaged over all grid cells within the dashed blue box over western Russia [48°–66° N, 22° –50° E] (right panel in Figure 1 of the main text).

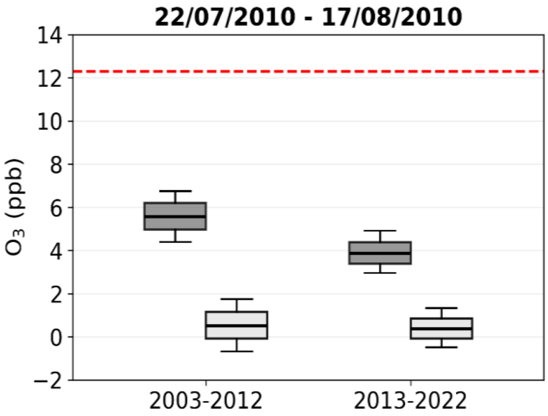

Figure S10. Distributions of the daily maximum ozone exceedances averaged over the target region in western Russia during 22 July – 17 August 2010 (right panel of Figure 1), reconstructed from flow analogues (dark grey boxes) and random (light grey boxes) distributions. Results are presented separately for two subperiods: 2003–2012 and 2013–2022 (x-axis). The red line represents the regional mean observed ozone exceedances during the episode.

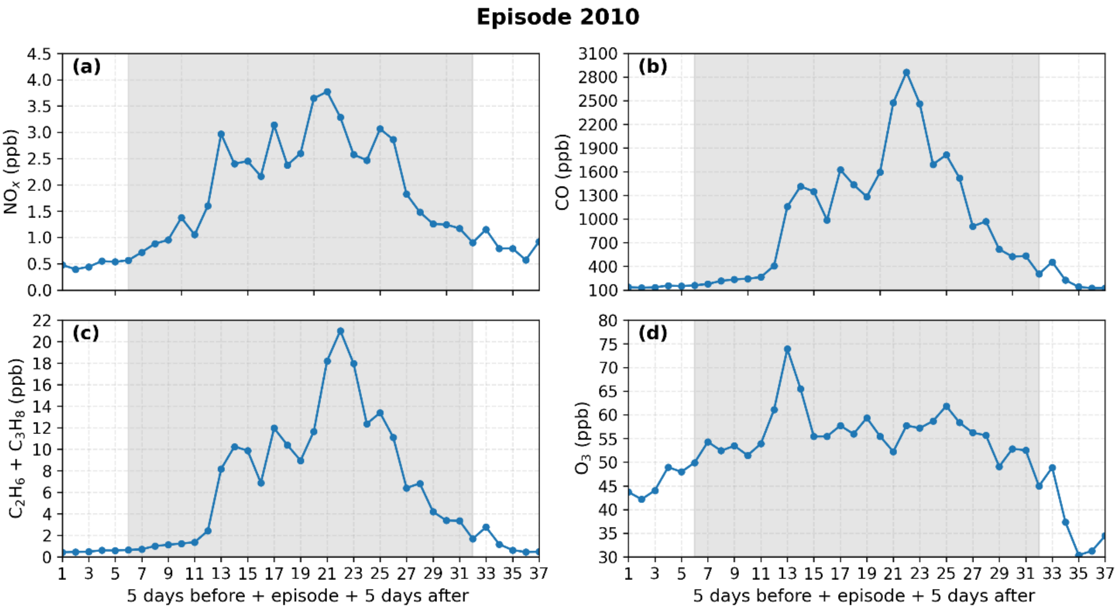

Figure S11. Temporal evolution of mixing ratios for (a) NO_x, (b) CO, and (c) anthropogenic NMVOCs (calculated as the sum of $C_2H_6 + C_3H_8$) at daytime (averages of 12 and 15 UTC values), as well as (d) daily ozone maxima (O_3), averaged over the target region during the episode that affected western Russia in summer 2010. The days of the episode (22 July – 17 Aug 2010, grey shading) as well as five days before the beginning and after the end of the episode are shown.

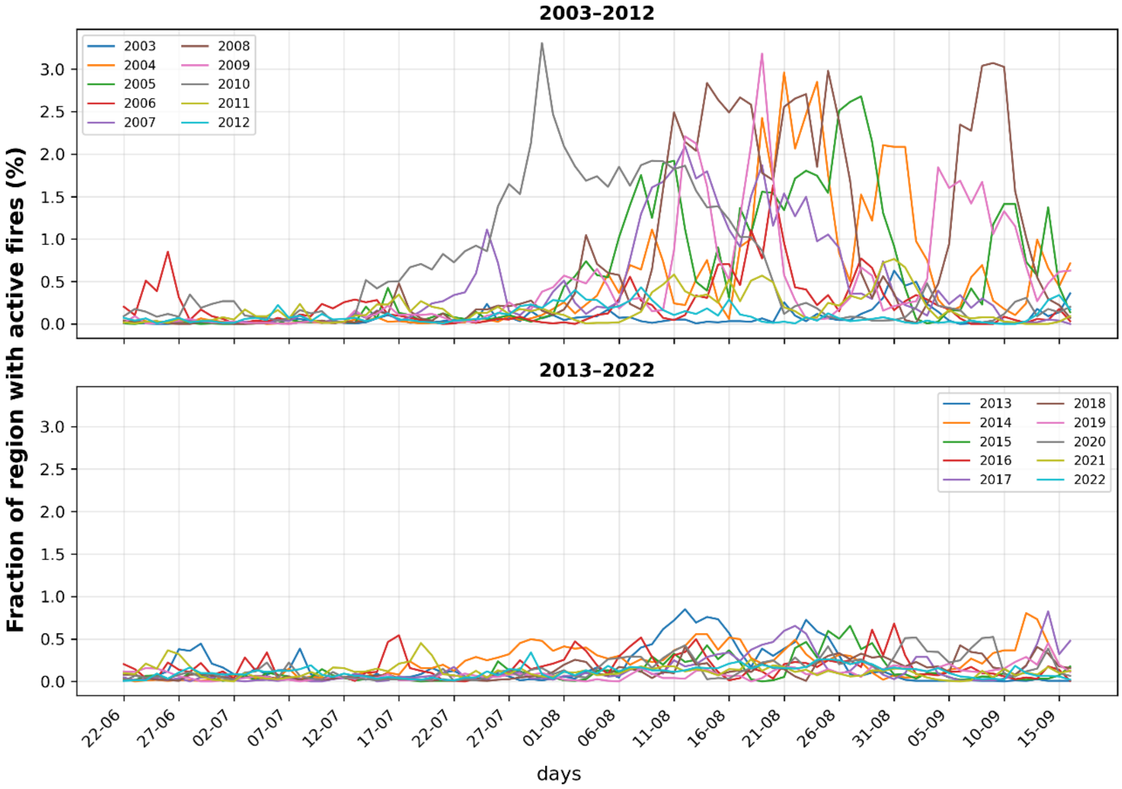

Figure S12. Yearly time series of the percentage of grid cells within the black box in the right panel of Figure 1 (July–August episode in western Russia) affected by biomass burning from the 22 June to 16 September periods of 2003–2022, separately for two different decades: (top) 2003–2012 and (bottom) 2013–2022.